

See discussions, stats, and author profiles for this publication at: <https://www.researchgate.net/publication/351758386>

Three Tank System Sensors and Actuators Faults Detection Employing Unscented Kalman Filter

Conference Paper · April 2021

DOI: 10.1109/PEMC48073.2021.9432611

CITATION

1

READS

103

5 authors, including:



Waseem Elsayed

University of Twente

33 PUBLICATIONS 126 CITATIONS

[SEE PROFILE](#)



Ahmed Aboelhassan

University of Nottingham Ningbo China

15 PUBLICATIONS 89 CITATIONS

[SEE PROFILE](#)



Ahmed Hebala

University of Nottingham

21 PUBLICATIONS 227 CITATIONS

[SEE PROFILE](#)



Giampaolo Buticchi

University of Nottingham Ningbo China

306 PUBLICATIONS 6,417 CITATIONS

[SEE PROFILE](#)

Some of the authors of this publication are also working on these related projects:



Highly Efficient and Reliable Smart Transformer (HEART) [View project](#)



Conceptual design methodology for evaluation of alternate fuel modifications on commuter category aircraft [View project](#)

Three Tank System Sensors and Actuators Faults Detection Employing Unscented Kalman Filter *

Waseem El Sayed
Electrical Engineering, Mathematics &
Computer Science (EEMCS),
University of Twente, Enschede, Netherlands.
w.wafiksaadelsayed@utwente.nl

Giampaolo Buticchi
Key Laboratory of More Electric Aircraft Technology of Zhejiang Province, University of Nottingham, Ningbo, China.
Giampaolo.Buticchi@nottingham.edu.cn

Ahmed Aboelhassan
Key Laboratory of More Electric Aircraft Technology of Zhejiang Province,
University of Nottingham, Ningbo, China.
Ahmed.Aboelhassan@nottingham.edu.cn

Ahmed Hebala
PEMC Group
University of Nottingham,
Nottingham, UK
Ahmed.hebala@nottingham.ac.uk

Michael Galea
Key Laboratory of More Electric Aircraft Technology of Zhejiang Province, University of Nottingham, Ningbo, China.
Michael.Galea@nottingham.edu.cn

Abstract — Fault detection is critical for industrial applications to maintain a stable operation and to reduce maintenance costs. Many fault detection techniques have been introduced recently to cope with the increasing demand for more safe operations. One of the most promising fault detection algorithms is the Unscented Kalman Filter (UKF). UKF is a model-based algorithm that could be used to detect different fault types for a given system. On the other hand, the three-tank system is a well-known benchmark that simulates many industrial applications. The fault detection of the three-tank system is quite challenging as it is a Multi-Input Multi-Output (MIMO) nonlinear system. Therefore, UKF will be employed as a fault detection strategy for this system to detect sensor and actuator faults. The performance of the UKF will be investigated under different operating and fault conditions to show its merits for the given case study.

Keywords — Fault detection, Three-tank system, Unscented Kalman Filter (UKF)

I. INTRODUCTION

Fault detection and tolerance are gaining more interest recently especially for industrial dynamic systems. This is primarily because of the increasing demand for improved control system performance, in addition to higher safety and reliability standards [1]. Faults can originate from the main process elements such as sensors or actuators [2]. This can be noticed as an error in the accuracy of level, temperature, or flow measurements. Also, it could be represented by uncalibrated or defective actuators such as motors and valves [3], [4].

Fault detection is roughly categorized into model-based and model-free methods. As the name suggests, model-free methods do not require the mathematical model of the process. However, a state-space model is usually used for the model-based methods or the transfer function model in some cases [5]. The model parameters are required to be well identified and known. Unfortunately, some of the system parameters could be either unknown or it is hard to be identified. It is necessary to have a comprehensive knowledge of these parameters to describe and analyze the system's dynamics. The unavailable system parameters can disturb the control system performance, the diagnostic algorithms, and degrade the overall system reliability and safety. Such abnormalities when occurred occasionally make the system faults occur [6].

The interest of this paper is using a model-based method, which can be sub-divided into state vs parameter estimation approaches. Although the parameters are of great importance as stated above, obtaining an exact value can be quite challenging. Therefore, one of the approaches is to formulate the parameter estimation as a state estimation problem by defining the fault parameter as an additional state. In the traditional Kalman Filter (KF) approach, the states are estimated through two distinct steps. First, the healthy state model is developed, then the faulty state one. The fault is estimated by analyzing the plant model mismatch [7], however, the parameters estimation errors increase with the system uncertainty. So, the Unscented Kalman Filter (UKF) is introduced as a modified version of the KF such that the mathematical state-space model is used to get a precise estimation of the fault parameters [8]. Therefore using UKF can overcome some of the EKFs weaknesses, such as the requirement of differentiable state dynamics, and sensitivity to bias or divergence in the state estimates [9].

A three-tank system is used as a case study for this paper. It represents a typical system in the process industry, such as the fuel management system of airplanes and flight vehicles as well as applications in chemical and petrochemical industries. It is considered a valuable experimental setup for studying multivariable feedback control as well as fault diagnosis [10]–[12]. Some of the main parameters of this system such as the viscosity coefficients are uncertain due to the change in the liquid characteristics, aging effects, other environmental reasons as corrosion, scaling, and changing operating conditions. Some techniques have been previously proposed such as neural, fuzzy [13], [14], non-linear observers [15], the generalized likelihood ratio-based system [16], and the multiple model-based approaches [17]. Nevertheless, these approaches are unable to estimate the fault if the noise in the system is higher than the fault magnitude. The proposed UKF can estimate the faults with low magnitude compared to the presented noise in the system. Additionally, UKF utilizes the method of the direct nonlinear model as an alternative to linearizing it [9]. This eliminates the need to calculate Jacobian or Hessian. Also, it has a further advantage of a lower computational burden.

The paper structure is as follows: the three-tank system state-space model is given in Section II. Section III is devoted to the adaptation of the three-tank system model by the UKF approach. Results are presented in Section IV for sensor and actuator faults considering the noise effect and tuning the covariance and weighting matrices. The performance is

* This work is funded by the INNOVATIVE doctoral programme. The INNOVATIVE programme is partially funded by the Marie Curie Initial Training Networks (ITN) action (project number 665468) and partially by the Institute for Aerospace Technology (IAT) at the University of Nottingham, UK.

evaluated at different operating conditions to test the system's robustness. Finally, the conclusions are highlighted in Section V.

II. THREE TANK SYSTEM MATHEMATICAL MODEL

The three-tank system is illustrated in Fig. 1. It includes similar cylinder-shaped tanks with a cross-section area A_t . The tanks are linked through two cylindrical tubes of cross-section area A_p with similar outflow coefficients μ_{13} and μ_{32} . The outflow is placed at the second tank with a cross-section area A_p with an outflow coefficient μ_{20} . Two pumps supply the first and second tanks, while the third tank affects their levels. q_1 and q_2 are the flow rates of the pumps with a maximum value of Q_{\max} . The system could be described by the following flow balance equations (1)-(3) [18], [19]:

$$A_t \frac{dL_1}{dt} = q_1(t) - q_{13}(t) \quad (1)$$

$$A_t \frac{dL_2}{dt} = q_2(t) + q_{32}(t) - q_{20}(t) \quad (2)$$

$$A_t \frac{dL_3}{dt} = q_{13}(t) - q_{32}(t) \quad (3)$$

where q_{mn} are the flow rate from tank m to tank n ($m, n = 1, 2, 3$ and $m \neq n$), L_1 , L_2 , and L_3 are the three-tank levels. Based on Torricelli law the flow rate equals (4):

$$q_{mn}(t) = \mu_{mn} A_p \operatorname{sign}(L_m(t) - L_n(t)) \sqrt{2g(L_m - L_n)} \quad (4)$$

where g is the gravity constant. Consequently, the flow rate for the three tanks will be (5)-(7):

$$q_{13} = \mu_{13} A_p \sqrt{2g(L_1 - L_3)} \quad (5)$$

$$q_{32} = \mu_{32} A_p \sqrt{2g(L_3 - L_2)} \quad (6)$$

$$q_{20} = \mu_{20} A_p \sqrt{2g(L_2)} \quad (7)$$

Thus, the flow balance equations for the first tank will be (8) and (9):

$$A_t \frac{dL_1}{dt} = q_1(t) - q_{13}(t) \quad (8)$$

$$A_t \frac{dL_1}{dt} = q_1(t) - \mu_{13} A_p \sqrt{2g(L_1 - L_3)} \quad (9)$$

for the second tank the flow balance equation is written as (10) and (11):

$$A_t \frac{dL_2}{dt} = q_2(t) + q_{32}(t) - q_{20}(t) \quad (10)$$

$$A_t \frac{dL_2}{dt} = q_2(t) + \mu_{32} A_p \sqrt{2g(L_3 - L_2)} - \mu_{20} A_p \sqrt{2g(L_2)} \quad (11)$$

and for the third tank rewritten as (12) and (13):

$$A_t \frac{dL_3}{dt} = q_{13}(t) - q_{32}(t) \quad (12)$$

$$A_t \frac{dL_3}{dt} = \mu_{13} A_p \sqrt{2g(L_1 - L_3)} - \mu_{32} A_p \sqrt{2g(L_3 - L_2)} \quad (13)$$

As a result, the three-tank system model could be written as:

$$\mathbf{x}(t) = \mathbf{r}(\mathbf{x}(t)) + \mathbf{s}(\mathbf{x}(t)) \mathbf{u}(t) \quad (14)$$

$$\mathbf{y}(t) = \mathbf{x}(t) \quad (15)$$

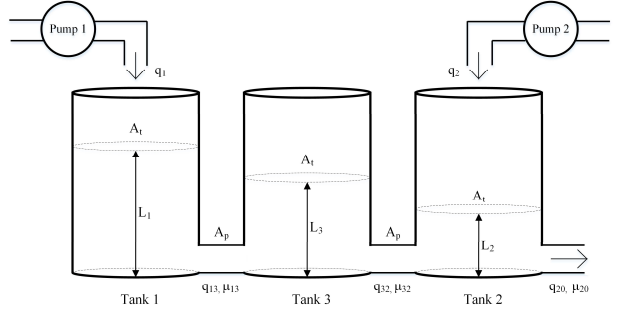


Fig. 1. Three-tank system.

where

$$\mathbf{r}(\mathbf{x}(t)) = \begin{bmatrix} -q_{13}(t) \\ A_t \\ \frac{q_{32}(t) - q_{20}(t)}{A_t} \\ \frac{q_{13}(t) - q_{32}(t)}{A_t} \end{bmatrix} = \begin{bmatrix} -\mu_{13} A_p \sqrt{2g(L_1 - L_3)} \\ A_t \\ \frac{\mu_{32} A_p \sqrt{2g(L_3 - L_2)} - \mu_{20} A_p \sqrt{2g L_2}}{A_t} \\ \frac{\mu_{13} A_p \sqrt{2g(L_1 - L_3)} - \mu_{32} A_p \sqrt{2g(L_3 - L_2)}}{A_t} \end{bmatrix}$$

$$\mathbf{s}(\mathbf{x}(t)) = \begin{bmatrix} \frac{1}{A_t} & 0 \\ 0 & \frac{1}{A_t} \\ 0 & 0 \end{bmatrix}$$

$$\mathbf{x}(t) = [L_1 \ L_2 \ L_3]^T, \mathbf{u}(t) = [q_1(t) \ q_2(t)]^T$$

If the presence of sensors' fault is considered, the sensor measurement does not equal the actual value, consequently, the output of the state space model will be:

$$\mathbf{y}(t) = \mathbf{x}(t) + \mathbf{F}_y(t) \quad (16)$$

where

$$\mathbf{y}(t) = \begin{bmatrix} L'_1 \\ L'_2 \\ L'_3 \end{bmatrix} = \begin{bmatrix} L_1 \\ L_2 \\ L_3 \end{bmatrix} + \begin{bmatrix} \Delta L_1 \\ \Delta L_2 \\ \Delta L_3 \end{bmatrix}$$

L'_1 , L'_2 and L'_3 are the measured values from the sensors and ΔL_1 , ΔL_2 and ΔL_3 are the differences between the actual and measured values.

In the case of the actuator faults, the fault appears in the input flow rates of the system pumps flow rates $q_1(t)$ and $q_2(t)$. The change in the flow rates could be represented in the added values to the nominal ones Δq_1 and Δq_2 . The state equation will be:

$$\mathbf{x}(t) = \mathbf{r}(\mathbf{x}(t)) + \mathbf{s}(\mathbf{x}(t)) \mathbf{u}(t) + \mathbf{F}_x(t) \quad (17)$$

where

$$\mathbf{F}_x(t) = \begin{bmatrix} \Delta q_1 \\ \Delta q_2 \\ 0 \end{bmatrix}^T$$

III. UNSCENTED KALMAN FILTER PROCEDURES

In the same framework, the procedures for implementing the UKF are presented in this section.

a) The System Model Extending

To estimate the fault in the three-tank system using UKF, the model states should be extended by the required unknown parameters, which is hard to be measured or determined by

sensors. In particular, the states of the three-tank system will be extended by five parameters:

$$\tilde{\mathbf{x}}(t) = [L'_1 \ L'_2 \ L'_3 \ \Delta L_1 \ \Delta L_2 \ \Delta L_3 \ \Delta q_1 \ \Delta q_2]^T \quad (18)$$

The added estimated parameters are represented by λ_k . The discrete extended model can be expressed as:

$$\begin{cases} \tilde{\mathbf{x}}_{k+1} = \mathbf{r}_k + s_k \mathbf{u}_k + F_{x_k} \lambda_k + \mathbf{w}_k \\ \tilde{\mathbf{y}}_k = \tilde{\mathbf{x}}_k + F_{y_k} \lambda_k + \mathbf{v}_k \end{cases} \quad (19)$$

where

$$\begin{aligned} \mathbf{r}_k &= \begin{bmatrix} 1 + T_s \cdot \mathbf{r}(\lambda_k) \\ \lambda_k \end{bmatrix}, s_k = \begin{bmatrix} T_s \cdot s(\lambda_k) \\ 0_{5 \times 2} \end{bmatrix} \\ F_{x_k} &= [s_k \ 0_{8 \times 3}], F_{y_k} = [I_{3 \times 3} \ 0_{3 \times 2}] \end{aligned}$$

b) Unscented Kalman Filter

For Kalman filter algorithms, UKF is a modified version of the Extended Kalman Filter (EKF). They are designed to deal with non-linear systems models in the presence of state and measurement noises. However, the UKF works with the concept of calculating the sigma point instead of using the Jacobian matrix for linearizing the non-linear model as in EKF [8]. The UKF procedure is stated in [8], the first step is the initialization of the parameters based on the initial values of the states $\hat{\mathbf{x}}_0^a$ and the covariance matrix P_0^a [20]:

$$\hat{\mathbf{x}}_0^a = [\hat{\mathbf{x}}_0^a \ 0 \ 0] \quad (20)$$

$$P_0^a = E[(\mathbf{x}_0^a - \hat{\mathbf{x}}_0^a)(\mathbf{x}_0^a - \hat{\mathbf{x}}_0^a)^T] \quad (21)$$

$$X_{k-1}^a = [\hat{\mathbf{x}}_{k-1}^a \ \hat{\mathbf{x}}_{k-1}^a \ \pm \sqrt{\gamma P_{k-1}^a}] \quad (22)$$

where γ is the states' dimension. The second step is calculating the sigma points of the states X_{k-1}^a based on (20) and expressed as:

$$\hat{\mathbf{x}}_k^- = \sum_{i=0}^{2L} W_i^m X_{i,k|k-1}^x \quad (23)$$

$$\hat{\mathbf{y}}_k^- = \sum_{i=0}^{2L} W_i^m Y_{k|k-1,i,k|k-1} \quad (24)$$

where W_i^m and W_i^C are weighting factors and they are equal to $1/2(\gamma)$. As in the EKF, the prediction phase is the next step for calculating the new covariance matrix P_k . It can be expressed as:

$$P_k^- = \sum_{i=0}^{2L} W_i^C (X_{i,k|k-1}^x - \hat{\mathbf{x}}_k^-)(X_{i,k|k-1}^x - \hat{\mathbf{x}}_k^-)^T \quad (25)$$

Finally, the measurement update equations where the Kalman gain K_k is calculated for the correction of the next state estimation $\hat{\mathbf{x}}_k$ and covariance matrix P_k is given by:

$$K_k = (P_{\hat{\mathbf{x}}_k^- \hat{\mathbf{y}}_k^-}) (P_{\hat{\mathbf{y}}_k^- \hat{\mathbf{y}}_k^-})^{-1} \quad (26)$$

$$\hat{\mathbf{x}}_k = \hat{\mathbf{x}}_k^- + K_k (\mathbf{y}_k - \hat{\mathbf{y}}_k^-) \quad (27)$$

$$P_k = P_k^- + K_k (P_{\hat{\mathbf{y}}_k^- \hat{\mathbf{y}}_k^-}) K_k^T \quad (28)$$

where $P_{\hat{\mathbf{y}}_k^- \hat{\mathbf{y}}_k^-}$ and $P_{\hat{\mathbf{x}}_k^- \hat{\mathbf{y}}_k^-}$ represent the covariance of the posterior sigma points of $\hat{\mathbf{y}}_k^-$ and $\hat{\mathbf{x}}_k^- \hat{\mathbf{y}}_k^-$ and expressed as:

$$P_{\hat{\mathbf{y}}_k^- \hat{\mathbf{y}}_k^-} = \sum_{i=0}^{2L} W_i^C (Y_{i,k-1} - \hat{\mathbf{y}}_k^-)(Y_{i,k-1} - \hat{\mathbf{y}}_k^-)^T \quad (29)$$

$$P_{\hat{\mathbf{x}}_k^- \hat{\mathbf{y}}_k^-} = \sum_{i=0}^{2L} W_i^C (X_{i,k|k-1}^x - \hat{\mathbf{x}}_k^-)(Y_{i,k-1} - \hat{\mathbf{y}}_k^-)^T \quad (30)$$

c) Covariance and weighting matrices tuning

The tuning of the weighting matrices, Q_k and R_k , depends on the amount of the state and measurement noises in the system. Consequently, both matrices are diagonal in terms of the standard deviation variance of the state noise σ_u^2 and measurements noises σ_y^2 . Based on [21], the Q_k and R_k are illustrated as:

$$\begin{cases} Q_k = \left(\frac{\partial \mathbf{r}_k}{\partial u_k} \right)^2 \cdot \sigma_u^2 \cdot \begin{bmatrix} I_m & 0 \\ 0 & \frac{q_\lambda}{q_x} \cdot I_n \end{bmatrix} \\ R_k = \sigma_y^2 \cdot I_m \end{cases} \quad (31)$$

where m is the number of states x and n is the number of estimated parameters λ . The ratio q_λ/q_x is equal to:

$$\frac{q_\lambda}{q_x} \approx \left(T_s / \left(\beta \sqrt{\sum_{i=1}^n \left(\left| \frac{\partial \mathbf{r}_{k_i}}{\partial x_k} \right|^2 \right)} \right) \right)^2 \quad (32)$$

where β is the evaluation time constant of the estimated parameters and i represents the number of the estimated parameters. It is a factor that can be used to set the value of q_λ/q_x . Applying (32) to (31), the initial value of the error covariance matrix and weighting matrices are given in (33):

$$\begin{aligned} P_0 &= [I_{8 \times 8}] \times 10^{-2} & R_k &= [I_{3 \times 3}] \times 10^{-2} \\ Q_k &= \begin{bmatrix} [1 \times 10^{-9}]_{3 \times 3} & 0 & 0 \\ 0 & [0.01]_{3 \times 3} & 0 \\ 0 & 0 & [1 \times 10^{-12}]_{2 \times 2} \end{bmatrix} \end{aligned} \quad (33)$$

IV. SIMULATION RESULTS AND DISCUSSION

The MATLAB/ Simulink program is used to simulate the process of the three-tank system. The system parameters and operating point are shown in Table I [11]. The sampling time T_s was chosen equal to 0.1 s. A closed loop PID control was implemented to the system with suitable gains that have been tuned based on the system model. The PID gains for both inputs are illustrated in Table II. The sensor and actuator faults are included and the UKF response is tested in both cases with and without considering the system noise.

a) UKF estimation response without the system noise

In this context, the UKF is tested without including the state or measurement noises, so it is considered as a noise-free operating condition for both types of system faults. The time constant for the parameter estimation β is chosen to be 0.1 s for all results in this case. β has a low value to increase the estimation response as much as possible, as the noise is not considered in these fault sceneries.

TABLE I. THREE TANK SYSTEM PARAMETERS

Parameter	Value
Tank cross-section area (A_t)	0.0154 m^2
Pipe cross-section area (A_p)	$5 \times 10^{-5} \text{ m}^2$
Outflow coefficient (μ_{mn})	$\mu_{13} = \mu_{32} = 0.5, \mu_{20} = 0.675$
Maximum flow rate constraint (Q_{max})	$1.2 \times 10^{-4} \text{ m}^3/\text{Sec}$
Maximum level (L_{max})	0.62 m
Operating point	$Q_1 = 0.35 \times 10^{-4} \text{ m}^3/\text{s}$ $Q_2 = 0.375 \times 10^{-4} \text{ m}^3/\text{s}$ $L_1 = 0.4 \text{ m}$ $L_2 = 0.2 \text{ m}$ $L_3 = 0.3 \text{ m}$

TABLE II. PID PARAMETERS VALUES.

Parameter	Value
Proportional gain (K_p)	28.78
Integral gain (K_i)	2.4
Differential gain (K_d)	-13.89

1) Sensors' fault

In such a scenario, the sensor faults are represented in adding an amount to the level measurement, which is undetermined by the utilized sensor. At $t = 250$ s, a decrease in the first tank level by 0.03 m is applied. The sensor still has the same reading without any change. The UKF estimates the actual level L_1 as one of the estimated states in the process as shown in Fig. 2. Consequently, the UKF calculates the difference between both readings ΔL_1 , which in this case is 0.03 m as shown in Fig. 3. The same scenario is applied for the second tank but as an increase in the actual level value of 0.04 m. This amount is not considered by the sensor reading L_2 as shown in Fig. 4. The UKF obtains the value of ΔL_2 and it is equal to -0.04 m as shown in Fig. 5. The estimation response is very fast for both cases of sensor faults, it takes 4 s to reach the steady-state, and the values of the estimated parameters are error-free.

2) Actuators' fault

In this case, the actual value of the level sensors L'_n is equal to the measured value L_n in all three-tank level measurements and the fault will occur at the feeding pumps of the system. The impact of the fault will appear in the input flow rates values of the system. An increase at the flow rate Q_1 by 50 % of its nominal value at $t = 250$ s will be imposed. The applied closed-loop control for the system will maintain the first tank level to its reference value as shown in Fig. 6. Consequently, The UKF estimates the added values to the flowrate difference Δq_1 as shown in Fig. 7. Another test is executed by reducing the flowrate Q_2 by 20 % at $t = 250$ s as shown in Fig. 8. The UKF evaluates the value of Δq_2 which causes a reduction in the flow rate Q_2 as presented in Fig. 9. The estimation response for both cases of actuator faults takes 8 s to reach steady-state and values of the estimated parameters are without error as it is a noise-free case.

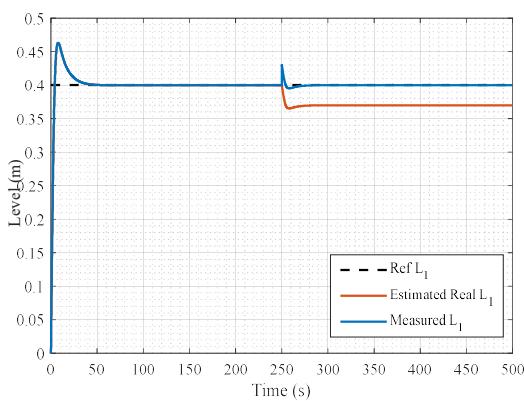


Fig. 2. The estimated actual value for the first tank level.

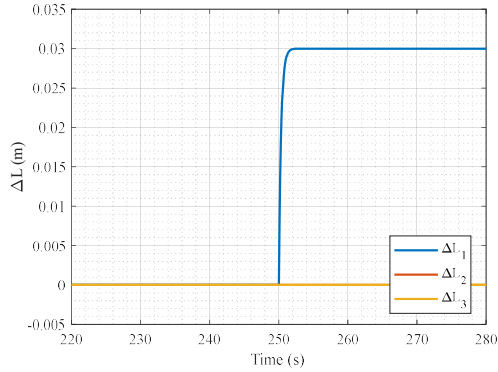


Fig. 3. The estimation response of ΔL for the first tank sensor fault.

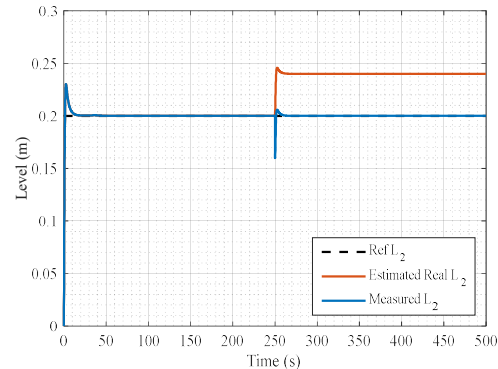


Fig. 4. The estimated actual value of the second tank level.

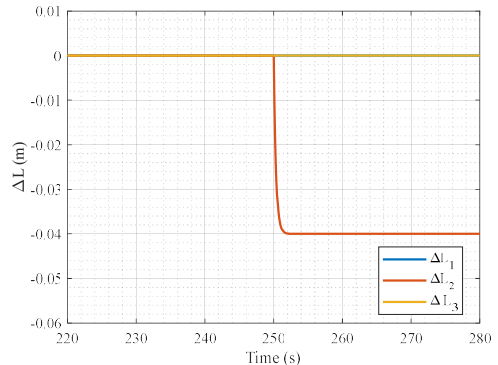


Fig. 5. The estimation response of ΔL for the second tank sensor fault.

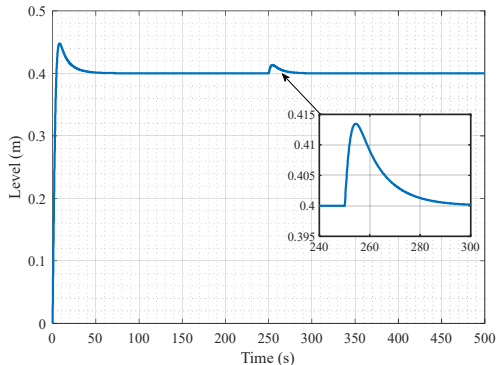


Fig. 6. The output measured level L_1 in presence of the first pump fault.

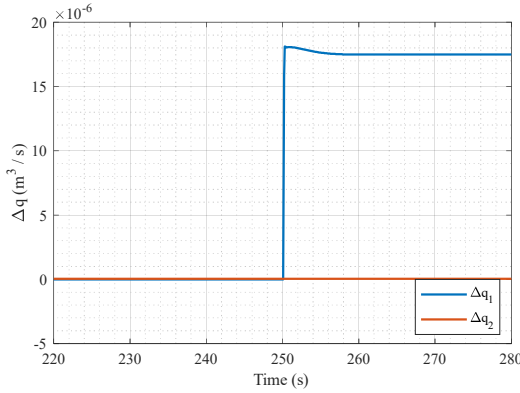


Fig. 7. The estimation response of Δq_1 for the first pump fault.

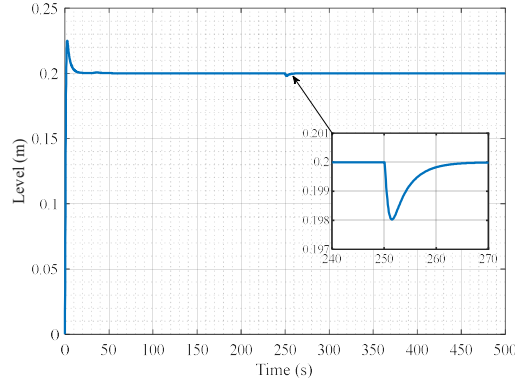


Fig. 8. The output measured level L_2 for the second pump fault.

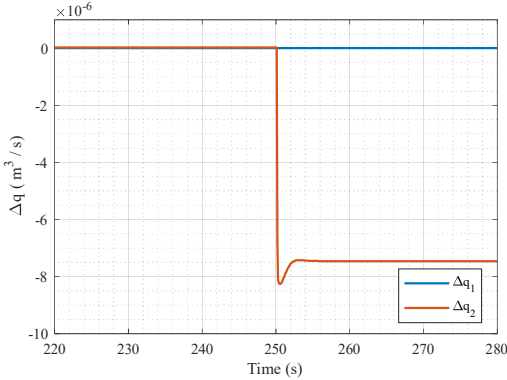


Fig. 9. The estimation response of Δq_2 for the second pump fault.

b) UKF estimation response considering the system noise

In order to simulate the real operating conditions, a white measurement noise with a standard deviation of 0.01 is added to the measured signal from the level sensors. In this case, the estimation response is affected by the added noise and the weighting matrices, Q_k and R_k , is very important for the estimation response performance. The tuning of the weighting matrices depends on the expected values of the measurements and output noise in the system. Thus, for the proposed case, the evaluation time constant β is chosen to be 100 s to deliver a suitable estimation response.

1) Sensors' fault

Fig. 10 shows the UKF estimation response of $\Delta L_1 = 0.05$ m considering an imposed fault at $t = 250$ s. The noise effect appears clearly in the estimation response time. The estimation reaches the steady-state after 118 s and the value

of the estimation tolerance is around 0.05 m. In this case, the mean value of the calculated error from the estimated signal for 1000 data points, which represents 100 s, is 1 %. The fault is repeated at various values for different tank levels and they have the same response as shown in Table III.

2) Actuators' fault

Similarly, at the same noise condition, an increase in the flow rate Q_1 by 50% of the operating point is occurred, the UKF estimates the value of Δq_1 after 125 s, and the estimation tolerance is around the added value as shown in Fig. 11. The percentage of the mean value of the calculated error from the estimated signal for 1000 data points is 7 %. The fault is repeated for flow rate Q_2 with different values of Δq , and the estimation of the UKF shows the same response as shown in Table IV.

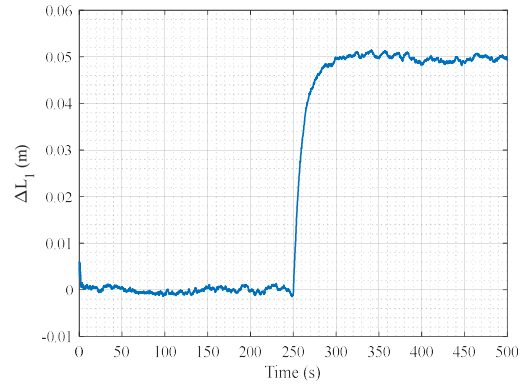


Fig. 10. The Estimation of ΔL_1 at $\beta = 100$ s for the level sensor fault at the noisy operating condition.

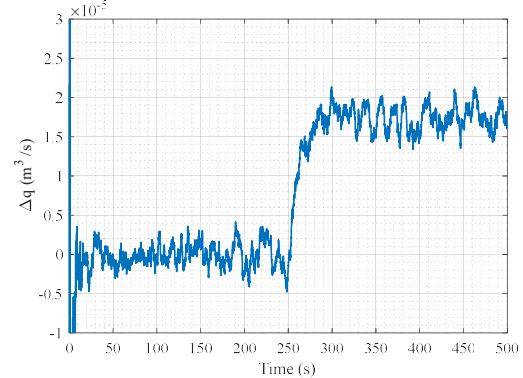


Fig. 11. The estimation response of Δq_1 at $\beta = 100$ s for the first pump fault at the noisy operating condition.

TABLE III. UKF ESTIMATED ΔL VALUES

Case	Reference value of ΔL_n (m)	Estimated $\Delta L_1, \Delta L_2, \Delta L_3$ (m)
1	0.01	0.0105
2	0.02	0.0205
3	0.03	0.0305
4	0.04	0.0404
5	0.05	0.0505
6	0.06	0.0605
7	0.07	0.0711
8	0.08	0.0805
9	0.09	0.0904
10	0.1	0.1005

TABLE IV. UKF ESTIMATED Δq VALUES

Case	Reference Δq_1 value (m^3/s)	Estimated Δq_1 (m^3/s)	Reference Δq_2 value (m^3/s)	Estimated Δq_2 (m^3/s)
1	$10\% \times Q_1$ (3.5×10^{-6})	4.7×10^{-6}	$10\% \times Q_2$ (3.75×10^{-6})	5.02×10^{-6}
2	$20\% \times Q_1$ (7×10^{-6})	8.212×10^{-6}	$20\% \times Q_2$ (7.5×10^{-6})	8.8×10^{-6}
3	$30\% \times Q_1$ (10.5×10^{-6})	11.71×10^{-6}	$30\% \times Q_2$ (11.2×10^{-6})	12.6×10^{-6}
4	$40\% \times Q_1$ (14×10^{-6})	15.21×10^{-6}	$40\% \times Q_2$ (15×10^{-6})	16.3×10^{-6}
5	$50\% \times Q_1$ (17.5×10^{-6})	18.71×10^{-6}	$50\% \times Q_2$ (18.7×10^{-6})	20×10^{-6}

3) The weighting matrices tuning

The change in the weighting matrices, Q_k and R_k , affect both the estimation time response and the percentage of the estimation error. Fig. 12 shows the effect of changing the evaluation time constant β in the estimation response. It is noticed that the increase in β of the estimated parameters is followed by a decrease in the parameters estimation error percentage as shown in Fig. 13 and Fig. 14. However, the estimation time response increases with the increase of β as illustrated in Fig. 15. The estimation error and time in the case of sensors' fault is less than the actuators' fault case due to the difference in the values of the estimated parameters.

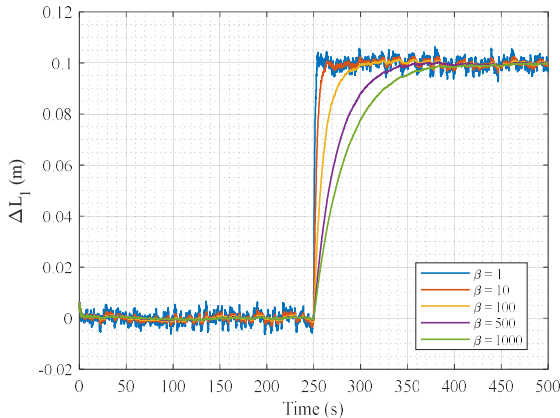
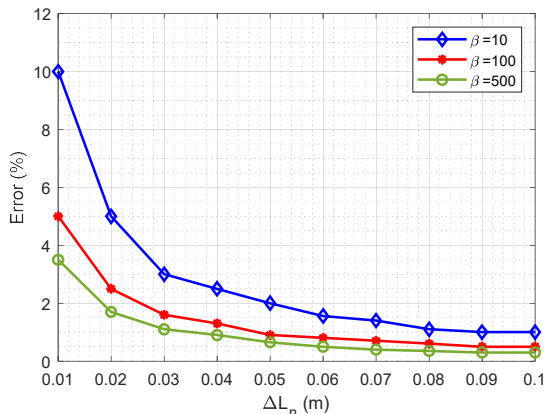
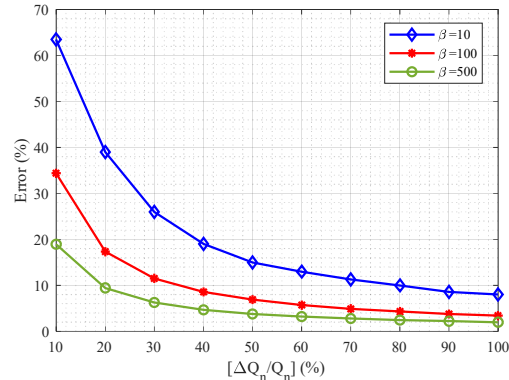
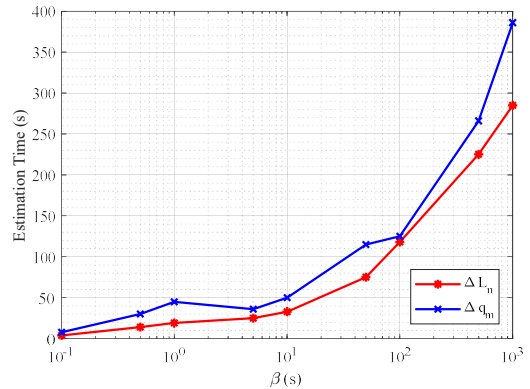
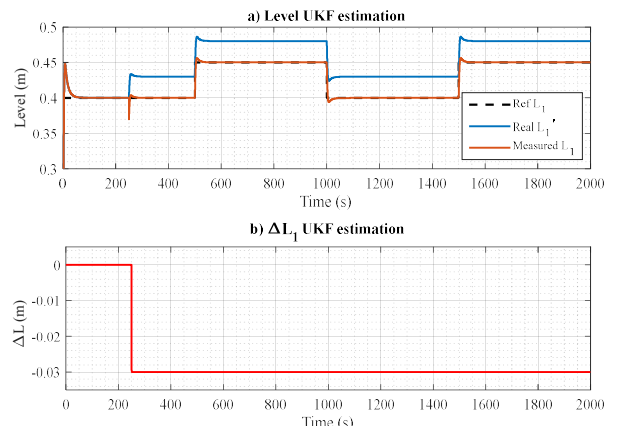

 Fig. 12. The estimation response of ΔL_1 at different values of β .

 Fig. 13. Error index for the sensor fault at different values of β .

 Fig. 14. Error index for the actuator fault at different values of β .


Fig. 15. Time index for the estimated parameters.

C) UKF estimation response with multi-operating points

To assure the successful operation of the studied technique in various operating conditions, the first tank level reference is step changed every 500 s without noise in the presence of a sensor false reading of $\Delta L_1 = -0.03$ m applied at $t = 250$ s as shown in Fig. 16a. The UKF shows constant estimation response with the change of the operating point as shown in Fig. 16b. Likewise, the UKF has a constant estimation response for the level and flow rate difference in the case of the first pump fault of $\Delta q_1 = 17.5 \times 10^{-6}$ as illustrated in Fig. 17.


 Fig. 16. The estimation response of ΔL_1 under various operating points.

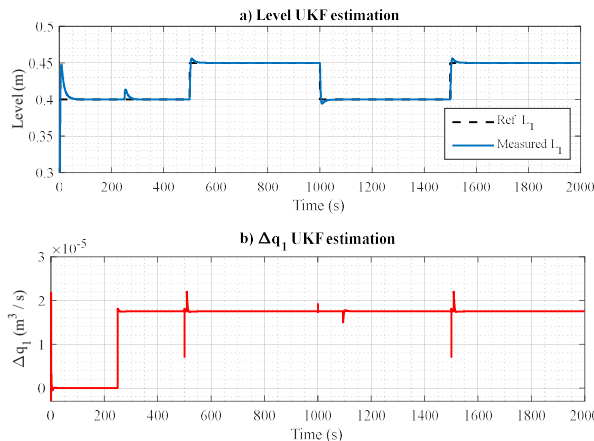


Fig. 17. The estimation response of Δq_1 under various operation points.

V. CONCLUSION

In this paper, the UKF technique has been presented as a fault diagnosis tool for industrial sensors and actuators faults. The three-tank system model has been used as a case study. The mathematical state-space model of the system has been introduced to be utilized by the UKF Technique. The sensor faults have been represented as a difference between the actual reading and the measured sensor reading ΔL_n of the level sensors, while the actuator faults have been represented as a difference between the expected and the real flow rate Δq_m controlled by the system pumps. The technique has been employed for the fault diagnosis with and without system noise. In the noise-free condition, the UKF technique estimated the ΔL_n and Δq_m accurately without noticeable error in all working conditions and fault values. Also, the estimation response was tuned to reach the steady-state after 4 s in the case of sensor fault and 8 s for actuator fault. However, the parameter estimation error increased with higher system noise. Thus, the weighting matrices, Q_k and R_k , should be tuned to give a suitable estimation response. The evaluation time constant of the estimated parameters β has been used to tune the value of the Q_k matrix. Consequently, the estimation response accuracy and speed were adapted according to the expected measurement noise of the system. The estimation response in the presence of noise reached the steady-state after around 120 s in both faults' cases. Besides, the UKF provided a robust response for sensor and actuator faults employing different operating conditions. The future work includes the experimental validation of the given algorithm and proposing a Fault-Tolerant Control (FTC) action.

References

- [1] A. Hussain, A. Q. Khan, M. Abid, and M. Tufail, "On fault detection in coupled liquid three tank system using subspace aided data driven design," *Proc. - 2012 Int. Conf. Emerg. Technol. ICET 2012*, pp. 59–64, 2012, doi: 10.1109/ICET.2012.6375467.
- [2] G. Krishnamoorthy, P. Ashok, and D. Tesar, "Simultaneous sensor and process fault detection and isolation in multiple-input-multiple-output systems," *IEEE Syst. J.*, vol. 9, no. 2, pp. 335–349, 2015, doi: 10.1109/JSYST.2014.2307632.
- [3] Zhiwu Wang, Jingzhe Yang, Huiping Ye, and Wei Zhou, "A review of Permanent Magnet Synchronous Motor fault diagnosis," in *2014 IEEE Conference and Expo Transportation Electrification Asia-Pacific (ITEC Asia-Pacific)*, 2014, pp. 1–5, doi: 10.1109/ITEC-AP.2014.6940870.
- [4] T. Guo, S. Chang, Z. Chen, H. Huang, and J. Xu, "Fault Monitoring and Diagnosis of Actuators in Electromagnetic Valve-Train Based on Neural Networks Optimization Algorithm," *IEEE Access*, vol. 7, pp. 110616–110627, 2019, doi: 10.1109/ACCESS.2019.2933881.
- [5] D. Kim and D. Lee, "Fault Parameter Estimation Using Adaptive Fuzzy Fading Kalman Filter," *Appl. Sci.*, vol. 9, 2019.
- [6] M. Iqbal, A. I. Bhatti, S. Iqbal, and Q. Khan, "Parameter estimation based fault diagnosis of uncertain nonlinear three tank system using HOSM differentiator observer," *INMIC 2009 - 2009 IEEE 13th Int. Multitopic Conf.*, 2009, doi: 10.1109/INMIC.2009.5383150.
- [7] A. Abid, M. T. Khan, and J. Iqbal, "A review on fault detection and diagnosis techniques : basics and beyond," *Artif. Intell. Rev.*, no. 0123456789, 2020, doi: 10.1007/s10462-020-09934-2.
- [8] W. El Sayed, M. A. El Geliel, and A. Lotfy, "Fault Diagnosis of PMSM Stator Inter-Turn Fault Using Extended Kalman Filter and Unscented Kalman Filter," *Energies*, vol. 13, no. 2972, pp. 1–24, 2020, doi: 10.1109/icone345789.2020.9117536.
- [9] A. Mirzaee and K. Salahshoor, "Fault diagnosis and accommodation of nonlinear systems based on multiple-model adaptive unscented Kalman filter and switched MPC and H-infinity loop-shaping controller," *J. Process Control*, vol. 22, no. 3, pp. 626–634, 2012, doi: https://doi.org/10.1016/j.jprocont.2012.01.002.
- [10] M. H. Sobhani and J. Poshtan, "Observer-based fault detection and isolation of three-tank benchmark system," *Proc. - 2011 2nd Int. Conf. Control. Instrum. Autom. ICCIA 2011*, pp. 759–763, 2011, doi: 10.1109/ICCIautom.2011.6356755.
- [11] A. A. Abdelrauf, M. Abdel-Geliel and, and E. Zakzouk, "Adaptive PID Controller Based on Model Predictive Control," 2016.
- [12] X. He, Z. Wang, Y. Liu, L. Qin, and D. Zhou, "Fault-Tolerant Control for an Internet-Based Three-Tank System: Accommodation to Sensor Bias Faults," *IEEE Trans. Ind. Electron.*, vol. 64, no. 3, pp. 2266–2275, 2017, doi: 10.1109/TIE.2016.2623582.
- [13] R. Ettoouil, K. Chabir, and M. N. Abdelkrim, "Synergetic control for three-tanks system: A comparison with the sliding mode control," *18th Int. Conf. Sci. Tech. Autom. Control Comput. Eng. STA 2017*, vol. 2018-Janua, no. 2, pp. 641–646, 2018, doi: 10.1109/STA.2017.8314902.
- [14] Y. Zhang, Y. Zhang, Q. Fan, and L. Song, "A Novel Approach Based on Terminal Sliding Mode Control for Optimization of Nonlinear Systems," *IEEE Access*, vol. 8, pp. 186505–186513, 2020, doi: 10.1109/access.2020.3029866.
- [15] M. De Rozprza-Faygel, M. Buciakowski, and M. Witczak, "Robust fault and state estimation for Lipschitz systems: Three-tank system application," in *2015 20th International Conference on Methods and Models in Automation and Robotics, MMAR 2015*, 2015, pp. 483–488, doi: 10.1109/MMAR.2015.7283923.
- [16] E. Elbouchikhi, Y. Amirat, G. Feld, and M. Benbouzid, "Generalized likelihood ratio test based approach for stator-fault detection in a PWM inverter-fed induction motor drive," *IEEE Trans. Ind. Electron.*, vol. 66, no. 8, pp. 6343–6353, 2019, doi: 10.1109/TIE.2018.2875665.
- [17] A. M. Bardawily, M. Abdel-Geliel, M. Tamazin, and A. A. A. Nasser, "Sensors fault estimation, isolation and detection using MIMO extended Kalman filter for industrial applications," *2017 10th Int. Conf. Electr. Electron. Eng. ELECO 2017*, vol. 2018-Janua, no. January 2018, pp. 944–948, 2018.
- [18] A. Aboelhassan, M. Abdelgeliel, E. E. Zakzouk, and M. Galea, "Design and Implementation of Model Predictive Control Based PID Controller for Industrial Applications," *Energies*, vol. 13, no. 24, p. 6594, Dec. 2020, doi: 10.3390/en13246594.
- [19] H. Noura, D. Theilliol, J.-C. Ponsart, and A. Chamseddine, *Fault-tolerant Control Systems*. 2009.
- [20] K. Zawirski, D. Janiszewski, and R. Muszynski, "Unscented and extended Kalman filters study for sensorless control of PM synchronous motors with load torque estimation," *Bull. POLISH Acad. Sci. Tech. Sci.*, vol. 61, no. 4, 2013, doi: 10.2478/bpasts-2013-0086.
- [21] B. Aubert, J. Regnier, S. Caux, and D. Alejo, "Kalman-Filter-Based Indicator for Online Interturn Short Circuits Detection in Permanent-Magnet Synchronous Generators," *Ind. Electron. IEEE Trans.*, vol. 62, no. 3, pp. 1921–1930, 2015, doi: 10.1109/TIE.2014.2348934.